# Investigation of InSAR Coherence Data and Frequency Ratio for Analyzing Forest Fires: A Case Study of Yamanlar, Izmir

Göktuğ Yaşar Çukurlu [1], Nusret Demir [2,3], Pol Kolokousis [4], Fulya Aydin-Kandemir [5], Ecmel Erlat [6]

[1] Akdeniz University, The Institute of Natural and Applied Sciences, Department of Space Science and Technologies 07258 Konyaaltı Antalya, Türkiye – 202351045003@ogr.akdeniz.edu.tr
[2] Akdeniz University, Faculty of Science, Department of Space Science and Technologies 07058 Konyaaltı Antalya, Türkiye - nusretdemir@akdeniz.edu.tr
[3] Eten R&D Ltd., Antalya Teknokent, 07070, Konyaaltı, Antalya, Türkiye
[4] National Technical University of Athens, Remote Sensing Laboratory, 15780 Athens, Greece, pol@survey.ntua.gr
[5] Climate Change and Zero Waste Department, Antalya Metropolitan Municipality, 07310, Türkiye – fulya.kandemir@antalya.bel.tr
[6] Department of Geography, Ege University, Izmir, 35100 Türkiye – ecmel.erlat@ege.edu.tr

**Keywords:** Coherence, Sentinel-1, Forest Fire, Histogram, InSAR, Frequency Ratio.

**Abstract**

Optical sensors are widely used in the detection and analysis of forest fires. However, in regions affected by dense smoke clouds during fires or areas with persistently cloudy weather due to climatic conditions, conducting analyses using optical imagery becomes challenging. Therefore, this study focuses on the detection and monitoring of forest fires using InSAR Coherence data. Prior to the fire detection/monitoring analyses, forest fire incidents in the Turkey/İzmir region between 2012 and 2024 were collected from the NASA FIRMS platform. In addition to these data, maps of slope, aspect, curvature, and drainage were derived from the DEM of the İzmir region. Urban areas in İzmir were identified using CORINE data, road networks were obtained from OSM datasets, temperature and wind data were retrieved from ERA-5 datasets, and precipitation data were sourced from the CHIRPS dataset. Using these collected parameters, forest fire susceptibility maps for the İzmir region were generated through the Frequency Ratio method. The resulting map revealed a direct correlation between increasing slope and heightened forest fire susceptibility in the region. Additionally, the urban parameter demonstrated a high frequency ratio in the analyses, indicating its contribution to fire risk, and areas near settlements were observed to exhibit high-risk levels on the map. Following the generation of the fire susceptibility map, a forest fire in the İzmir/Yamanlar Mountain area was investigated using the InSAR Coherence method. The analyses showed that forest fires can be detected/monitored through the changes observed in InSAR Coherence histograms and coherence-based maps. Furthermore, it was observed that the application of a threshold value to the coherence histogram enabled the classification of forested areas in the region.

## 1. Introduction

Fire is a natural hazard that profoundly alters terrestrial ecosystems, playing a critical ecological role across much of the Earth's surface. It is well-documented that fires reduce soil fertility, alter water supplies, decrease biomass, increase biodiversity loss, adversely impact carbon sequestration, and disrupt surface radiation balance, causing global-scale damage (Belenguer-Plomer et al., 2019; Liu et al., 2019; Stoyanova et al., 2022). Forests burned due to natural or anthropogenic causes have become a significant concern, with increasingly frequent "megafires" escalating in scale. This escalation is closely linked to shifts in temperature, precipitation, and humidity driven by intensifying global climate change (Aydin-Kandemir & Demir, 2023). Moreover, forested areas degraded by climate change likely contribute to the process itself, suggesting that forest fires are trapped in a cycle of mutual reinforcement (Calfee & Little, 2003; Majlingová, 2012).

Although intervening in this cycle is challenging, mitigating its effects and analyzing fire risk remain feasible. Frequency Ratio analysis can generate fire susceptibility maps by calculating the frequency ratio of fire occurrences within the value ranges of relevant factors, providing a spatial representation of fire susceptibility (Tiwari et al., 2021).

In August 2024, a forest fire in the Yamanlar Mountain region of Izmir, Turkey, affected approximately 3,500 hectares. This study has two objectives: (1) detect and monitor the evulation of a forest fire using InSAR coherence histograms and imagery, and (2) generate a fire susceptibility map for the region to assess future fire risk.

The InSAR coherence method allows for fire detection even under the presence of dense smoke, a common obstacle in fire monitoring. This study utilizes coherence values from the Sentinel-1 SAR (Synthetic Aperture Radar) sensor, an active sensor operating at a C-band frequency of 5.405 GHz (Torres et al., 2012). This C-band sensor can penetrate the forest canopy (Udali et al., 2021), and as an active sensor, it is unaffected by day/night cycles or atmospheric conditions like smoke and clouds (www.asf.alaska.edu). Dense smoke from the Yamanlar Mountain fire hindered data acquisition from optical sensors like Sentinel-2 and Landsat-8, delaying damage assessment until after the fire was extinguished. In contrast, SAR sensors, through interferometry and coherence analysis, can detect changes in fire zones by comparing images taken at different times.

Coherence analysis examines the consistency of phase differences between SAR images. Seasonal factors, such as leaf growth and fall, influence coherence values, generally resulting in low coherence in forested areas due to the scattering of radio waves (Closson & Milisavljevic, 2017). We anticipate changes in coherence values due to fire-induced losses. This raises key questions:

- Can we obtain information about biomass changes in the region following forest fires by analyzing coherence values and fire intensity/area parameters?

- Can coherence histograms help determine the estimated severity of forest fires?

This study explores InSAR coherence maps and histograms as an alternative method for detecting forest fires and assessing their severity by monitoring their evulation. Sentinel-1 SAR data, unaffected by clouds and smoke (Tsai et al., 2020), allows for imaging during active fires and in cloudy conditions. The primary focus is analyzing InSAR data and coherence values, specifically the magnitude component which ranges from 0 (no correlation) to 1 (perfect correlation) (Abdel-Hamid et al., 2021), to determine fire severity.

## 2. Test Site and Methodology

This study investigates forest fire susceptibility in Izmir, Turkey, using frequency ratio analysis and InSAR coherence values to assess fire detectability.

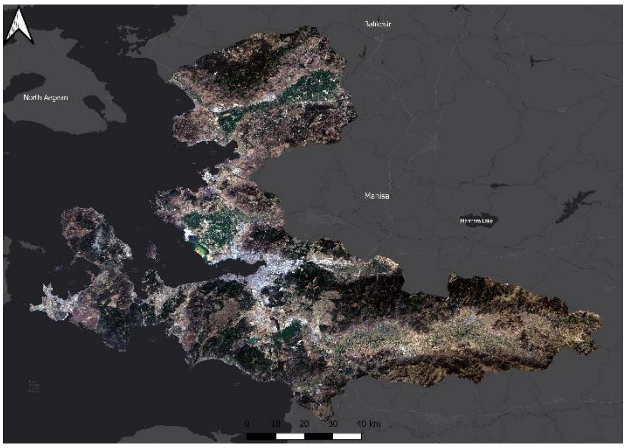


Figure 1. Study area map Turkey/ Izmir. Landsat-8 image over a ESRI dark basemap.

According to NASA FIRMS data, 157 fires with a power greater than 50 MW were identified in Izmir province between 2012 and 2024. In determining the number of these fires, a threshold value was applied to the collected NASA FIRMS data to select those exceeding 50 MW (Singh et al., 2022). In 2024, a forest fire occurred on Yamanlar Mountain in the Karşıyaka district of Izmir. According to news reports (Anadolu Agency), approximately 3,000 ha were damaged by the forest fire. Due to the frequent occurrence of forest fires in the region, the frequency ratio method was used to produce a fire susceptibility map and to determine the areas that may suffer the most damage in potential fires. The InSAR coherence histogram method was used for the Turkey/Izmir region to quickly detect fire in the event of a potential forest fire. Due to the frequent forest fires in the region, the frequency ratio method and the InSAR coherence histogram method have been employed to generate a fire sensitivity map based on frequency ratio and to identify areas most vulnerable to significant damage in potential fires (Lee & Pradhan, 2007). These methods were applied to the Turkey/Izmir region to rapidly detect fires in the event of a potential forest fire.

The parameters required to generate the fire sensitivity map using the frequency ratio include forest fire data for the Izmir region (2012-2024) obtained from the NASA FIRMS platform, DEM (Digital Elevation Model) data from the Google Earth Engine platform, urban area data from the CORINE methodology (2018), road network data from the OSM (OpenStreetMap) platform, and NDVI (Normalized Difference Vegetation Index) and NDMI (Normalized Difference Moisture Index) data generated using Landsat-8 satellite imagery. Wind and temperature data were acquired from the Copernicus Climate Service platform's ERA-5 dataset, while precipitation data were obtained from the CHIRPS platform. The selection of these parameters was guided by previous studies that used the frequency ratio method to produce fire sensitivity maps (Abdo et al., 2022; Youssef et al., 2015; Pham et al., 2020). The NDVI and NDMI (Equation 1, 2) were calculated for August (median image used for Landsat-8, NDVI, and NDMI) for Izmir.

$$NDVI = \frac{(NIR-R)}{(NIR+R)}, \tag{1}$$

where NDVI = Normalized Difference Vegetation Index
NIR = Near-infrared band reflectance
R = Red band reflectance

$$NDMI = \frac{(NIR-SWIR)}{(NIR+SWIR)}, \tag{2}$$

where NDMI = Normalized Difference Moisture Index
NIR = Near-infrared band reflectance
SWIR = Short-wave infrared band reflectance

$$TWI = ln\frac{(CA)}{(SLOPE)}, \tag{3}$$

where TWI = Topographic Wetness Index
CA = Local upscale basin area
Slope = Slope outlines (Tarboton, 1997).

For the other classes, 'Natural Breaks' was applied as a classification method (Abdo, et al., 2022). To calculate the frequency ratio, the frequency ratio formula was applied to each of the 13 parameters (Equation 4).

$$FR = \frac{(S/M)}{(Q/R)}, \tag{4}$$

where FR = Frequency Ratio
S = The number of forest fire events for each class of each motivated parameter
M = Overall forest fire events
Q = The number of pixels for each class of the criterion
R = The total number of pixels

After determining the frequency ratios for each class, the relevant classes were assigned to the values calculated by a Reclassification process, and forest fire susceptibility maps were produced with 'Weighted Sum'. Once the forest fire susceptibility maps were produced, the process steps given in Figure 2 were followed for the detection of forest fires using InSAR coherence histograms with the Sentinel-1 SAR (Synthetic Aperture Radar) (C-band) sensor.

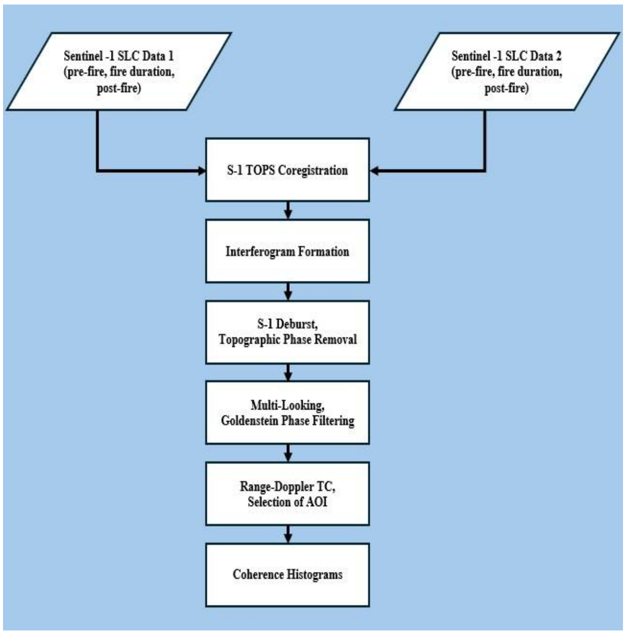


Figure 2. InSAR processing workflow diagram.

In all the process steps in the diagram given in Figure 2, the parameters were left as default. In this way, in case of a possible forest fire, the aim is to have information about the fire quickly and practically, without the need to specify extra parameters. InSAR coherence histograms were used for fire detection, while InSAR coherence-based maps were used to observe the fire area.

To create InSAR coherence for forest fires, data were collected from two different dates before the fire. The same process was then repeated during the fire, using two data points: one from before the fire and one during the fire. Finally, data were collected approximately two weeks after the fire for post-fire analysis. The ESA Sentinel Application Platform (SNAP), developed by the European Space Agency was used for InSAR coherence extraction. The IW2 route was used for the Izmir/Yamanlar Mountain region. Information was collected from alaska.asf. The prescribed protocols were implemented using SNAP. In the TOPS-SPLIT stage, Interferometric Wide Field (IW) data covering the specific region of interest were used. VV polarization was used to extract coherence from Sentinel-1 SLC data.

## 3. Results and Discussion

### 3.1 Frequency Ratio

Frequency Ratio analysis, which is among the geostatistical methods, is also used in the production of forest fire susceptibility maps by calculating the fire frequency ratio (FO) between the value ranges of related factors (Tiwari et al., 2021).

| Frequency Ratio Classes | | Very Low | Low | Moderate | High | Very High |
|---|---|---|---|---|---|---|
| Frequency Ratio Values | Slope | 0.16513 | 0.59646 | 1.14607 | 1.72071 | 4.41689 |
| Frequency Ratio Values | Aspect | 1.44307 | 1.28673 | 1.67835 | 1.34312 | 1.43541 |
| Frequency Ratio Values | DEM | 0.96052 | 1.2183 | 1.30978 | 0.13052 | 0.52644 |
| Frequency Ratio Values | Curvature | 2.68772 | 1.4419 | 0.63991 | 0.68168 | 1.40066 |
| Frequency Ratio Values | TWI | 0.75124 | 0.78566 | 0.48542 | 0.78086 | 2.70104 |
| Frequency Ratio Values | NDMI | 0.33623 | 0.45172 | 0.5059 | 1.20751 | 1.76515 |
| Frequency Ratio Values | NDVI | 0.58736 | 1.59442 | 1.45638 | 0.67832 | 0.52145 |
| Frequency Ratio Values | Drenage | 0.89938 | 0.71133 | 1.19071 | 0 | 0 |
| Frequency Ratio Values | Wind | 0.66937 | 4.83652 | 1.2403 | 2.42548 | 0 |
| Frequency Ratio Values | Roads | 0.67659 | 1.73908 | 1.40252 | 0 | 0 |
| Frequency Ratio Values | Urban | 0.30471 | 1.14895 | 1.4344 | 2.23386 | 0.79588 |
| Frequency Ratio Values | Temperature | 0 | 0.85168 | 0.32757 | 1.66763 | 0 |

Table 1. Frequency Ratio for every parameter.

Very Low: Represents areas with a very low frequency ratio and shows minimal association with fire occurrence. Low:
Represents areas with a low frequency rate and indicates a lower probability of fire occurrence.
Moderate: Represents areas with a medium frequency rate and indicates a moderate association with fire occurrence.
High: Represents areas with a high frequency rate: Represents areas with a high frequency rate and indicates a higher probability of fire occurrence.
Very High: Represents areas with a very high frequency rate and indicates a strong association with fire occurrence. The frequency rate increases with class, indicating a stronger association with fire occurrence in higher classes.


https://doi.org/10.5194/isprs-archives-XLVIII-M-6-2025-109-2025 | © Author(s) 2025. CC BY 4.0 License.

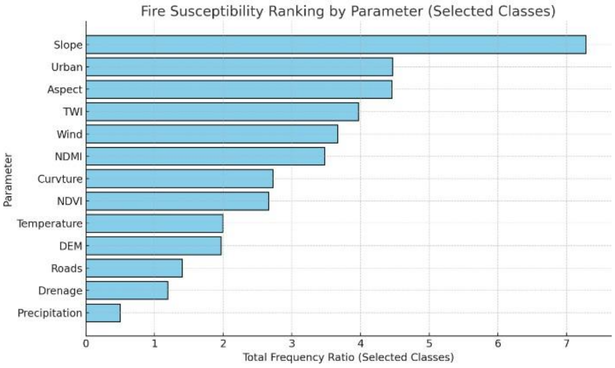


Figure 3. Total frequency ratios of Very High, High and Moderate classes.

As a result of the analysis, the most effective parameter in terms of fire susceptibility was determined to be slope. When the total frequency ratio in the Very High, High, and Moderate classes is evaluated, the slope parameter has the highest value. This shows that slope has a strong influence on fire occurrence and spread. Especially in sloping areas, wind effects and the concentration of combustible materials increase the risk of fire.

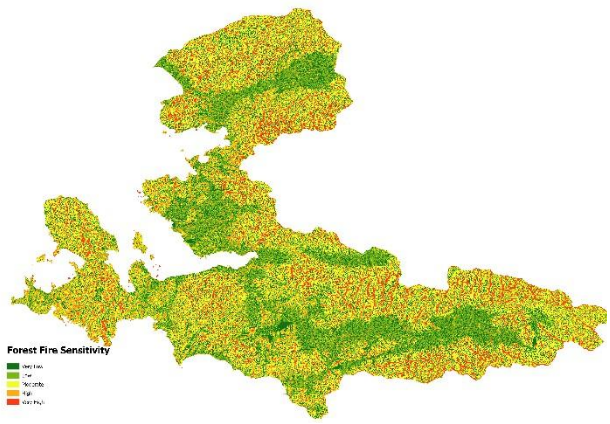


Figure 4. Forest fire susceptibility map generated with FR.

There is a relationship between the map produced and the analyses performed. The map geographically confirms the results obtained from the frequency ratio analysis of the parameters. Especially, the slope parameter stands out as one of the most critical factors in terms of fire susceptibility, both in the analysis and on the map. The fact that the red areas on the map are largely concentrated in steep slope areas clearly reveals the effect of slope on fire risk. In addition, the urban parameter has shown its contribution to fire risk with a high-frequency rate in the analyses, and it is observed that areas close to residential areas are also of high risk. The aspect parameter, on the other hand, contributes to fire susceptibility mainly by accounting solar irradiation, and this can be observed by the fact that the southern slopes appear as higher-risk areas.

The fire susceptibility value of each pixel was calculated by combining the frequency ratios in the analyses with the "Weighted Sum" method used in map generation. As a result, the map and analyses clearly reveal which areas are more critical in terms of fire risk and show that these areas should be addressed as a priority. In this context, the map provides a valuable guide for the geographical planning of fire prevention and response strategies. The results obtained with the FR method are consistent with the results obtained in previous studies (Tshering et al., 2020; Tuyen et al., 2021; Gholamnia et al., 2020).

### 3.2 InSAR Coherence Data

The success and consistency of the InSAR method, which is mostly used in deformation analysis, have been investigated in forest fires. Coherence values, which show the phase differences between two SAR data of different dates, allow InSAR to observe factors such as structures, objects, or terrain changes caused by earthquakes. Because of the variable structure in forested areas, the phases will be seen differently each time by the sensor. For example, the phase taken from the treetop in the first pass may be taken from a leaf of the tree in the next pass under the same conditions (Wei et al., 2024). In this context, coherence histograms showing the change between pre-fire and fire duration are expected since areas such as trees and shrubs in forested areas will be damaged during a fire. After the fire, since the wooded areas are damaged, constant phases will be recorded instead of different phases. In this context, while low coherence values are expected in forested areas before the fire, medium-high coherence values are expected after the fire.

In line with this information, SAR images in SLC format were collected to analyze the Izmir/Yamanlar Mountain forest fire with InSAR coherence data. The collected images are as given in Table 2.

| Date | Data Format | Path | Frame | Mode |
|---|---|---|---|---|
| 07/11/2024 | Single Look Complex | 36 | 462 | DESCENDING |
| 07/23/2024 | Single Look Complex | 36 | 462 | DESCENDING |
| 08/04/2024 | Single Look Complex | 36 | 462 | DESCENDING |
| 08/28/2024 | Single Look Complex | 36 | 462 | DESCENDING |
| 09/09/2024 | Single Look Complex | 36 | 462 | DESCENDING |
| 09/21/2024 | Single Look Complex | 36 | 462 | DESCENDING |
| 11/20/2024 | Single Look Complex | 36 | 462 | DESCENDING |
| 12/02/2024 | Single Look Complex | 36 | 462 | DESCENDING |

Table 2. Sentinel-1 Data types.

The eight data points given in Table 2 were analyzed in four different time periods. Data were analyzed for pre-fire detection with 11-23 July 2024 data, fire duration with 4-28 August data, post-fire with 9/21 September data, and post-fire regeneration detection with 20 November-2 December data. After applying the processing steps given in Figure 2 to the data, InSAR coherence data for forest fires were created. The fire area was selected from the coherence-based image, and histograms were extracted.

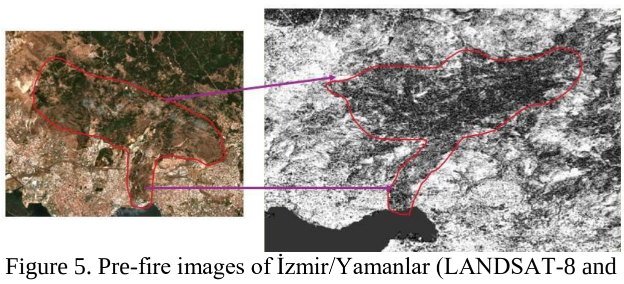

Figure 5. Pre-fire images of İzmir/Yamanlar (LANDSAT-8 and Sentinel-1 InSAR, respectively).

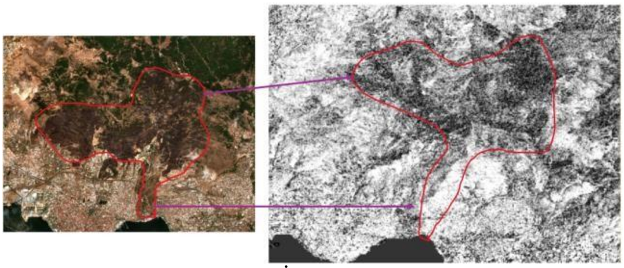

Figure 6. Post-fire images of İzmir/Yamanlar (LANDSAT-8 and Sentinel-1 InSAR, respectively.

When Figures 5 and 6 are analyzed, it is seen that forest fires are also detectable in InSAR coherence-based maps. This demonstrates that it is possible to observe forest fires with InSAR coherence-based maps in cases where optical sensors cannot provide data at the time of the fire, or the fire cannot be monitored by remote sensing systems due to dense smoke. At the same time, since InSAR coherence histograms are formed while creating these images, it is possible to detect forest fires with numerical analysis.

Figure 7. Regeneration images of İzmir/Yamanlar (LANDSAT-8 and Sentinel-1 InSAR, respectively.

When Figure 7 is examined, it is seen that there is a small regeneration in the area approximately three months after the fire. There is a strong correlation between the satellite image and the InSAR coherence-based image. With InSAR coherence, unlike the pure satellite image, the regenerated green areas in the region can be selected spatially through phase differences caused by the effect of scattering.

We also investigated the detectability of forest fires based on the coherence histograms obtained from coherence-based map generation. The results are given in Figures 8, 9, 10, and 11.

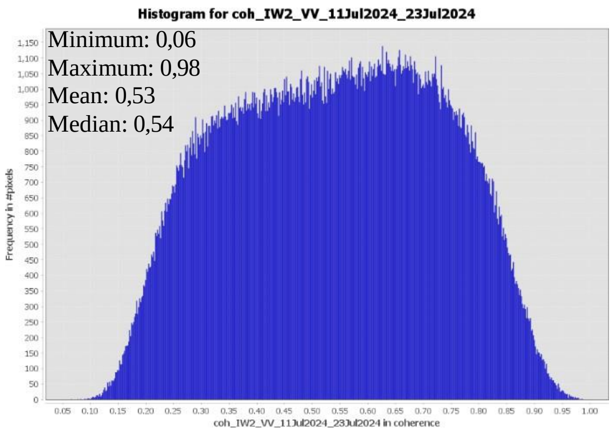


Figure 8. Pre-fire coherence values for Izmir/Yamanlar.

Analyzing the InSAR coherence histogram of the pre-fire data, we can observe low coherence values because of scattering from the trees. Since high coherence cannot be observed in the histogram, with an average value of 0.54 pixels, we can also interpret that it is a forested area. In Fig. 9, we observe a significant decrease in the InSAR coherence value because there will be a serious change in the region during the fire period. The main reason for this change is that the trees in the area before the fire started to burn during the fire. In this context, InSAR coherence values are expected to increase in the two datasets taken after the fire.

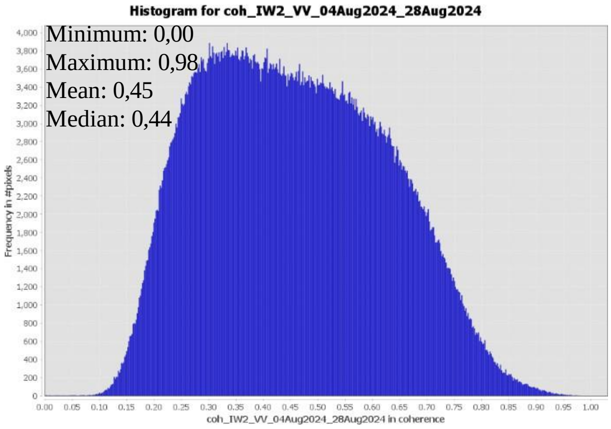


Figure 9. Fire duration coherence values for Izmir/Yamanlar.

The InSAR coherence-based map and histograms created with an image taken before the fire and an image taken during the fire showed a decrease, as expected. The main reason for this decrement is based on change in the region. Due to this decrease, the region colored with darker pixels in the coherence-based map allows us to actively identify the fire's location. At the same time, it has been observed that forest fires can also be detected with histograms, thanks to the difference between the histograms of the same region created before the fire.

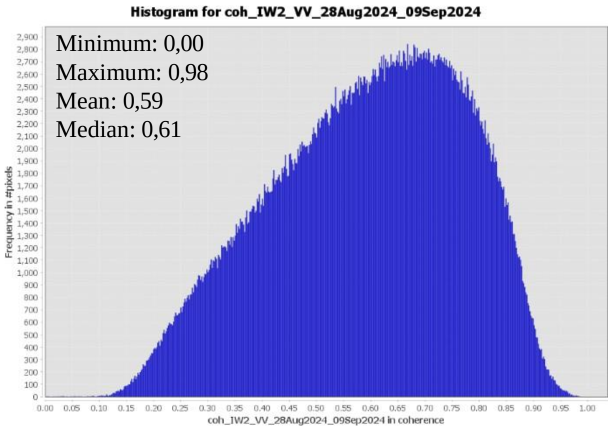


Figure 10. Post-fire coherence values for Izmir/Yamanlar.

Figure 10 shows that after the fire is extinguished, there will be a significant loss of trees and leaves in the forested areas, so the differences between the phases are reduced. In this figure, we observe that pixels have high values in the histogram displayed after the fire. Our results show that InSAR coherence values can effectively indicate forest fires.

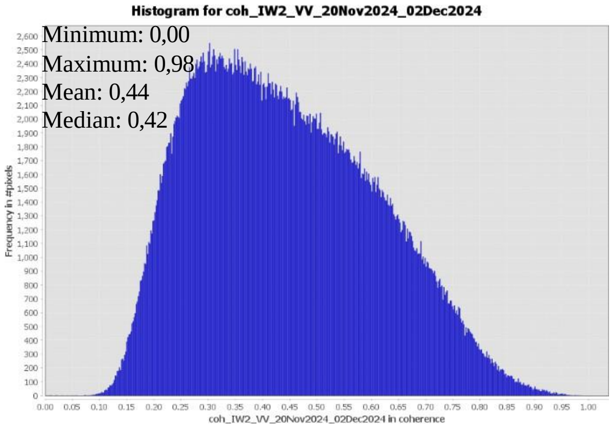


Figure 11. Post-fire coherence values for Izmir/Yamanlar.

In the InSAR coherence histogram created using two recent SAR data points, we observe a decrease in pixel values after the fire. This decrease indicates that regeneration has occurred in the region. This observation demonstrates that fire detection, as well as regeneration in the region, can be identified using InSAR coherence histograms.

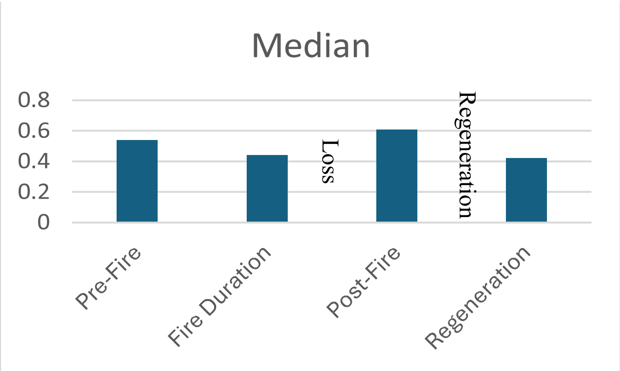


Figure 12. Median coherence values for Izmır/Yamanlar forest fire.

It is also possible to detect fires by plotting the changes in coherence values. When the graph is analyzed, we can observe the change in coherence values that occurred during and after the fire. When we examine the coherence values as of today, we can observe that regeneration has occurred.

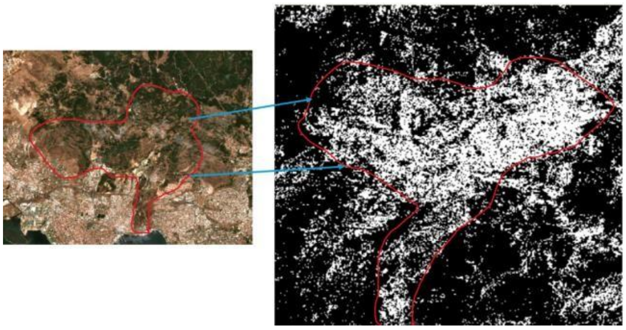

Figure 13. Median coherence values for Izmır/Yamanlar forest fire.

## 4. Conclusions

The InSAR coherence method demonstrates potential for detecting as well as monitoring the evulation of forest fires. Additionally, applying a threshold value to the low coherence values could enable forest area classification. In Fig. 13, a threshold value of 0.40 is applied. White pixels represent forested areas, while black pixels represent non-forested areas.

Future studies should investigate the InSAR coherence method for forest fire detection in regions with diverse climatic characteristics and tree structures. Consistent results obtained by examining changes in InSAR coherence histograms, in response to changes in the region or tree structures, would further support the accuracy and applicability of this method for forest fire detection and monitoring.

Combining forest fire susceptibility maps produced with Frequency Ratio analysis and InSAR coherence maps could enhance fire management strategies. Susceptibility maps can identify high-risk areas, while InSAR coherence maps could potentially predict fire spread direction, enabling proactive measures before a fire escalates.

This study explored both forest fire susceptibility mapping and forest fire detection using the InSAR coherence method. The results indicate that areas with steep slopes are at higher risk of fire spread. Furthermore, the InSAR coherence method shows promise as an alternative approach for forest fire detection and monitoring.

**Acknowledgements**

This study has been supported and financed by Scientific and Technological Research Council of Turkey (TUBITAK) with the Project Nr. 123Y274 with coordination and support from the COST Action CA20118.

**References**

Abdel-Hamid, A., Dubovyk, O., Greve, K., 2021. The potential of sentinel-1 InSAR coherence for grasslands monitoring in Eastern Cape, South Africa. *International Journal of Applied Earth Observation and Geoinformation*, 98. doi.org/10.1016/j.jag.2021.102306.

Abdo, H.G., 2022. Assessment of landslide susceptibility zonation using frequency ratio and statistical index: a case study of Al-Fawar basin, Tartous, Syria. *International Journal of Environmental Science and Technology*, 19(4), 2599-2618

Aydin-Kandemir, F., Demir, N., 2023. 2021 Turkey mega forest Fires: Biodiversity measurements of the IUCN Red List wildlife mammals in Sentinel-2 based burned areas. *Advances in Space Research*, 71(7), 3060-3075. doi.org/10.1016/j.asr.2023.01.031.

Belenguer-Plomer, M.A., Tanase, M.A., Fernandez-Carrillo, A., Chuvieco, E., 2019. Burned area detection and mapping using Sentinel-1 backscatter coefficient and thermal anomalies. *Remote Sensing of Environment*, 233. doi.org/10.1016/j.rse.2019.111345.

Calfee, R.D., Little, E.E., 2003. Effects of a fire-retardant chemical to fathead minnows in experimental streams. *Environmental Science and Pollution Research*, 10, 296-300.

Closson, D., Milisavljevic, N., 2017. InSAR Coherence and Intensity Changes Detection. In Mine Action - The Research Experience of the Royal Military Academy of Belgium. InTech. doi.org/10.5772/65779.

Lee, S., Pradhan, B., 2007. Landslide hazard mapping at Selangor, Malaysia using frequency ratio and logistic regression models. *Landslides*, 4(1), 33-41.

Liu, Z., Ballantyne, A.P., Cooper, L.A., 2019. Biophysical feedback of global forest fires on surface temperature. *Nature communications*, 10(1), 214.

Majlingová, A., 2012. Opening-up of forests for fire extinguishing purposes. *Croatian Journal of Forest Engineering: Journal for Theory and Application of Forestry Engineering*, 33(1), 159-168.

Pham, B.T., Jaafari, A., Avand, M., Al-Ansari, N., Dinh Du, T., Yen, H.P.H., ..., Tuyen, T.T., 2020. Performance evaluation of machine learning methods for forest fire modeling and prediction. *Symmetry*, 12(6), 1022. doi.org/10.3390/sym12061022.

Singh, M., Sharma, C., Agarwal, T., Pal, M.S., 2022. Forest fire prediction for nasa satellite dataset using machine learning. In *2022 10th International Conference on Reliability, Infocom Technologies and Optimization (Trends and Future Directions)(ICRITO)*, 1-5.

Stoyanova, J.S., Georgiev, C.G., Neytchev, P.N., 2022. Satellite Observations of Fire Activity in Relation to Biophysical Forcing Effect of Land Surface Temperature in Mediterranean Climate. *Remote Sensing*, 14(7), 1747. doi.org/10.3390/rs14071747.

Tiwari, A., Shoab, M. Dixit, A, 2021. GIS-based forest fire susceptibility modeling in Pauri Garhwal, India: a comparative assessment of frequency ratio, analytic hierarchy process and fuzzy modeling techniques. *Nat Hazards*, 105, 1189–1230. doi.org/10.1007/s11069-020-04351-8.

Torres, R., Snoeij, P., Geudtner, D., Bibby, D., Davidson, M., Attema, E., Potin, P., Rommen, B.Ö., Floury, N., Brown, M., Traver, I.N., Deghaye, P., Duesmann, B., Rosich, B., Miranda, N., Bruno, C., L’Abbate, M., Croci, R., Pietropaolo, A., …, Rostan, F., 2012. GMES Sentinel-1 mission. *Remote Sensing of Environment*, 120, 9–24. doi.org/10.1016/j.rse.2011.05.028.

Tsai, Y.L.S., Klein, I., Dietz, A., Oppelt, N., 2020. Monitoring large-scale inland water dynamics by fusing sentinel-1 sar and sentinel-3 altimetry data and by analyzing causal effects of snowmelt. *Remote Sensing*, 12(23), 1–30. doi.org/10.3390/rs12233896.

Udali, A., Lingua, E., Persson, H.J., 2021. Assessing forest type and tree species classification using sentinel-1 c-band sar data in southern Sweden. *Remote Sensing*, 13(16). doi.org/10.3390/rs13163237.

Yang, Y., Luo, Y., 2011. Carbon: nitrogen stoichiometry in forest ecosystems during stand development. *Global Ecology and Biogeography*, 20(2), 354-361.

Youssef, A.M., Al-Kathery, M., Pradhan, B., 2015. Landslide susceptibility mapping at Al-Hasher area, Jizan (Saudi Arabia) using GIS-based frequency ratio and index of entropy models. *Geosciences Journal*, 19, 113-134.

Tshering, K., Thinley, P., Shafapour Tehrany, M., Thinley, U., Shabani, F., 2020. A comparison of the qualitative analytic hierarchy process and the quantitative frequency ratio techniques in predicting forest fire-prone areas in Bhutan using GIS. *Forecasting*, 2(2), 36-58. doi.org/10.3390/forecast2020003.

Tuyen, T.T., Jaafari, A., Yen, H.P.H., Nguyen-Thoi, T., Van Phong, T., Nguyen, H.D., ..., Pham, B.T., 2021. Mapping forest fire susceptibility using spatially explicit ensemble models based on the locally weighted learning algorithm. *Ecological Informatics*, 63, 101292. doi.org/10.1016/j.ecoinf.2021.101292.

Gholamnia, K., Gudiyangada Nachappa, T., Ghorbanzadeh, O., Blaschke, T., 2020. Comparisons of diverse machine learning approaches for wildfire susceptibility mapping. *Symmetry*, 12(4), 604. doi.org/10.3390/sym12040604.

Wei, R., Deng, Z., Xiong, S., Zhang, B., Li, Q., 2024, July. Forest Canopy Height Estimation based on InSAR Coherence. In *IGARSS 2024-2024 IEEE International Geoscience and Remote Sensing Symposium*, 5402-5405.